Articles

Monopalmitoylphosphatidylcholine Incorporation into Human Erythrocyte Ghost Membranes Causes Protein and Lipid Immobilization and Cholesterol Depletion†

David E. Golan,*,‡,§,∥ Stephen T. Furlong,‡,⊥ Carl S. Brown,‡,§ and John P. Caulfield⊥,#

Departments of Medicine, Pathology, and Biological Chemistry and Molecular Pharmacology, Harvard Medical School, and Departments of Medicine (Hematology Division) and Rheumatology/Immunology, Brigham and Women's Hospital, Boston, Massachusetts 02115

Received September 15, 1987; Revised Manuscript Received December 9, 1987

ABSTRACT: The effects of lysophosphatidylcholine (lysoPC) on human erythrocyte (RBC) ghost morphology, transmembrane protein and lipid lateral mobilities, and membrane lipid composition were studied in order to elucidate mechanisms by which lysoPC immobilizes ghost membrane components [Golan, D. E., Brown, C. S., Cianci, C. M. L., Furlong, S. T., & Caulfield, J. P. (1986) *J. Cell Biol. 103*, 819–828]. Under standardized conditions 1.0–1.5 μg/mL egg lysoPC lysed 50% of RBCs and induced, in some ghosts, the formation of large patches of wrinkled membrane. Patches exhibited complete immobilization of glycophorin and band 3 and partial immobilization of the phospholipid analogue fluorescein phosphatidylethanolamine (Fl-PE), whereas adjacent smooth membrane areas manifested only partial immobilization of proteins and no immobilization of Fl-PE. Supralytic concentrations of lysoPC induced both progressive, homogeneous wrinkling of RBC ghost membranes and concentration-dependent decreases in the lateral mobilities of glycophorin, band 3, and Fl-PE. Complete immobilization of glycophorin and band 3 occurred at 8.4 μg/mL lysoPC and of Fl-PE at 16.8 μg/mL lysoPC. Monopalmitoylphosphatidylcholine (MPPC), the major component of egg lysoPC, induced both membrane wrinkling and a concentration-dependent decrease in Fl-PE mobility, with complete immobilization at 10 μg/mL. Other synthetic lysoPCs did not completely immobilize Fl-PE, although some caused membrane wrinkling. MPPC was incorporated into ghost membranes with a linear dependence ($r = 0.97$) on MPPC concentration. Relative to total membrane lipid, the lysoPC mole fraction increased from 0.2 ± 0.1% at 0 μg/mL MPPC to 25 ± 2% at 16 μg/mL MPPC. The molar ratio of cholesterol to phospholipid (exclusive of lysoPC) in MPPC-treated ghosts was inversely dependent on MPPC concentration, decreasing from 1.0 ± 0.1 at 0 μg/mL MPPC to 0.7 ± 0.2 at 8 μg/mL MPPC. This ratio did not decrease further at 12 and 16 μg/mL MPPC. MPPC treatment did not affect the relative amounts of the major RBC phospholipid classes. These results suggest that MPPC causes concentration-dependent changes in the composition and organization of RBC ghost membranes. LysoPC incorporation and/or cholesterol depletion may induce lipid domain formation, which causes membrane protein and lipid immobilization.

Lysophosphatidylcholine (lysoPC)[1] affects both model and biological membranes, including the human erythrocyte (RBC) membrane. At sublytic concentrations lysoPC makes RBCs echinocytic and increases RBC osmotic fragility, agglutinability, and membrane permeability. The rate and extent of lysis are dependent on RBC density, temperature, and both the molecular species and concentration of lysoPC [reviewed in Weltzien (1979)]. The mechanism of lysoPC-induced hemolysis is unclear. RBC membrane components may be extracted by lysoPC micelles, or the membrane architecture may be disrupted by lysoPC incorporation. Since hemolysis is slower than lysoPC binding to RBCs (Weltzien et al., 1976), a rearrangement of lysoPC within the membrane may precede hemolysis (Weltzien, 1979). Ghosts produced by lysoPC and fixed with glutaraldehyde exhibit 300-Å membrane defects and are permeable to ferritin (Seeman, 1967).

Supralytic concentrations of lysoPC may mediate important interactions between parasites and host blood cells. We have previously found that human RBCs adhere to and are lysed by schistosomula of *Schistosoma mansoni* (Caulfield &

† This work was supported by National Institutes of Health Grants AI15311, HL32854, AI19581, and AI23083. D.E.G. was a Fellow of The Medical Foundation, Inc. (Boston, MA), during the course of this work.

* Address correspondence to this author at the Department of Biological Chemistry and Molecular Pharmacology, Harvard Medical School, 250 Longwood Ave., Boston, MA 02115.

‡ Department of Medicine, Harvard Medical School.

§ Department of Biological Chemistry and Molecular Pharmacology, Harvard Medical School.

∥ Department of Medicine (Hematology Division), Brigham and Women's Hospital.

⊥ Department of Rheumatology/Immunology, Brigham and Women's Hospital.

Department of Pathology, Harvard Medical School.

[1] Abbreviations: BSA, bovine serum albumin; cmc, critical micelle concentration; *D*, diffusion coefficient; EDTA, ethylenediaminetetraacetate; *f*, fractional mobility; Fl-PE, fluorescein phosphatidylethanolamine; FPR, fluorescence photobleaching recovery; hct, hematocrit; HPLC, high-performance liquid chromatography; lysoPC, lysophosphatidylcholine; MPPC, monopalmitoylphosphatidylcholine; MSPC, monostearoylphosphatidylcholine; MWG, moderately wrinkled ghost; PBS, phosphate-buffered saline; PC, phosphatidylcholine; PG, patchy ghost; PMSF, phenylmethanesulfonyl fluoride; RBC, erythrocyte; SG, smooth ghost; SWG, single-wrinkle ghost; VWG, very wrinkled ghost.

0006-2960/88/0427-2661$01.50/0

Cianci, 1985). These adherent RBC ghosts exhibit complete immobilization of the major integral membrane proteins, glycophorin and band 3, and partial immobilization of two lipid probes, fluorescein phosphatidylethanolamine (Fl-PE) and carbocyanine dyes. The latter finding is not duplicated by treatment of RBCs with membrane protein cross-linking agents. Immobilization of membrane proteins and lipids is found, however, in RBCs treated with supralytic concentrations of egg lysoPC. This phenomenon is not due to RBC lysis alone, since ghosts produced by hypotonic lysis do not exhibit membrane component immobilization. Further, schistosomula release sufficient amounts of metabolically labeled lysoPC into the culture medium to account for RBC lysis and membrane component immobilization. These data suggest that lysoPC is transferred from schistosomula to adherent RBCs, causing their lysis (Golan et al., 1986).

In the present study we have examined the effects of lysoPC on the morphology and lipid composition of RBC ghosts and on the lateral mobility of fluorescently labeled ghost proteins and lipids. Our goal was to elucidate mechanisms by which supralytic concentrations of egg lysoPC immobilize ghost membrane components. Egg lysoPC was found to induce the formation of morphologically distinct regions, called wrinkles and patches, in ghosts. Membrane proteins and lipids were immobilized in both wrinkled ghosts and patchy areas of patchy ghosts. Monopalmitoylphosphatidylcholine (MPPC), the major component of egg lysoPC, was also found to induce wrinkling and immobilization. This synthetic lysoPC was therefore employed in studies of the lipid composition of lysoPC-treated ghosts, and the results of these studies were compared with lateral mobility measurements on proteins and lipids in similarly treated ghosts. We have concluded that incorporation of MPPC and extraction of cholesterol are critical in MPPC-induced protein and lipid immobilization.

Materials and Methods

Reagents. Fl-PE, egg lysoPC, synthetic lysoPCs [monolauroyl- (C12:0), monomyristoyl- (C14:0), monopalmitoyl- (C16:0), monostearoyl- (C18:0), and monooleoyl-phosphatidylcholines (C18:1) (PCs)], brain phosphatidylserine, brain sphingomyelin, cholesterol, dioleoylphosphatidylethanolamine, dioleoyl-PC, and egg phosphatidic acid were from Avanti Polar Lipids, Inc. (Birmingham, AL). The fatty acid composition of egg lysoPC is 70.5% palmitic acid, 25.7% stearic acid, 1.8% oleic acid, and 0.7% palmitoleic acid (Avanti Polar Lipids, Inc., personal communication). RPMI-1640 culture medium was from Gibco Laboratories (Grand Island, NY). Bovine serum albumin (BSA) (essentially fatty acid and globulin free) was from Sigma Chemical Co. (St. Louis, MO). Disodium ethylenediaminetetraacetate (EDTA) was from Fisher Scientific Co. (Fair Lawn, NJ). Phenylmethanesulfonyl fluoride (PMSF) was from Eastman Organic Chemicals (Rochester, NY).

Preparation and Fluorescent Labeling of Human RBCs and RBC Ghosts. Fresh blood was washed 3 times by centrifugation in phosphate-buffered saline (PBS) (128 mM NaCl, 10 mM sodium phosphate, pH 7.4) with 120 μM PMSF and 1 mM EDTA and once in PBS. Glycophorin was labeled with fluorescein thiosemicarbazide, band 3 was labeled with eosin maleimide, and Fl-PE was incorporated in the membranes of washed RBCs as described (Golan et al., 1986).

In intact RBCs treated with supralytic concentrations of monopalmitoylphosphatidylcholine (MPPC), MPPC could bind to hemoglobin as well as to membranes. Such binding could complicate measurements of the lipid composition of MPPC-treated RBCs. Labeled or unlabeled RBCs were therefore lysed hypotonically and the resulting ghosts treated with MPPC. MPPC-treated ghosts were used in parallel studies of membrane morphology, lateral mobility, and lipid composition to determine whether MPPC treatment caused the same alterations in ghosts as in intact RBCs. RBCs were lysed in 40 volumes of 5 mM sodium phosphate with 120 μM PMSF and 1 mM EDTA, pH 7.4 (lysis buffer), for 45 min at 4 °C. Ghosts were washed 4 times by centrifugation in lysis buffer.

Incubation of Fluorescently Labeled RBCs and RBC Ghosts with LysoPC. Two protocols were employed. In the first protocol, 25 μL of packed, fluorescently labeled RBCs or ghosts was mixed with 12 mL of PBS and 0–20 μg/mL of egg or synthetic lysoPC from a freshly prepared stock solution of 10 mg/mL in H_2O. The mixture was vortexed for 1 min at 23 °C and washed twice in PBS and once in RPMI with 1% BSA (RPMI/BSA). In the second protocol, 25 μL of RBCs was mixed with 12 mL of RPMI and 0–8 μg/mL of egg lysoPC, vortexed for 5 s at 23 °C, incubated for 24 h at 37 °C, and washed twice in RPMI and once in RPMI/BSA. Samples were diluted in 10 volumes of RPMI/BSA, and 1-μL aliquots were sealed on RPMI/BSA-treated microscope slides for FPR experiments. Pretreatment with BSA prevented echinocyte formation in control RBC samples. LysoPC-induced changes in ghost morphology and membrane component lateral mobility were unaffected by substitution of PBS for RPMI as the incubation buffer and/or the FPR sample buffer.

Fluorescence Microscopy and Photomicrography. Fluorescently labeled RBCs and ghosts were examined by phase contrast and fluorescence microscopy, using an Orthoplan microscope (E. Leitz, Inc., Rockleigh, NJ). Cells were photographed with a Leitz Vario-Orthomat camera using Kodak Tri-X film exposed at 1600 ASA and developed with Diafine (Acufine, Inc., Chicago, IL).

Fluorescence Photobleaching Recovery (FPR). The lateral mobility of glycophorin, band 3, and Fl-PE in fluorescently labeled RBC membranes was measured by FPR (Axelrod et al., 1976). In this technique, a single-cell membrane is observed in a fluorescence microscope using a focused laser beam as the excitation source. A small area of membrane is exposed to a brief, intense laser pulse, causing irreversible bleaching of the fluorophore in that area. Fluorescence recovery resulting from lateral diffusion of unbleached fluorophore into the bleached area is measured. Analysis of fluorescence recovery curves yields the fraction of fluorescently labeled protein or lipid that is free to diffuse in the plane of the membrane (the mobile fraction, f), as well as the diffusion coefficient (D) of the mobile fraction.

Our FPR apparatus and analytical methods have been described in detail (Golan et al., 1986). The Gaussian beam radius at the sample plane, as determined by a two-dimensional emission scan technique (A. H. Stolpen, C. S. Brown, and D. E. Golan, submitted for publication), was 0.53 ± 0.02 μm. Photobleaching power at the sample was approximately 2 mW. Bleaching times were typically 40 ms for protein diffusion measurements and 5 ms for lipid diffusion measurements. Sample temperatures were controlled to 23.0 ± 0.1 °C by using a thermal microscope stage.

Lipid Composition of Monopalmitoyl-PC-Treated RBC Ghosts. Washed, packed ghosts (50 μL) were mixed with 24 mL of PBS and 0–16 μg/mL MPPC from a freshly prepared stock solution of 2 mg/mL in H_2O. The mixture was vortexed for 1 min at 23 °C and washed twice in PBS, and the resulting pellets were stored at −20 °C. The lipid composition of MPPC-treated ghosts was determined by high-performance

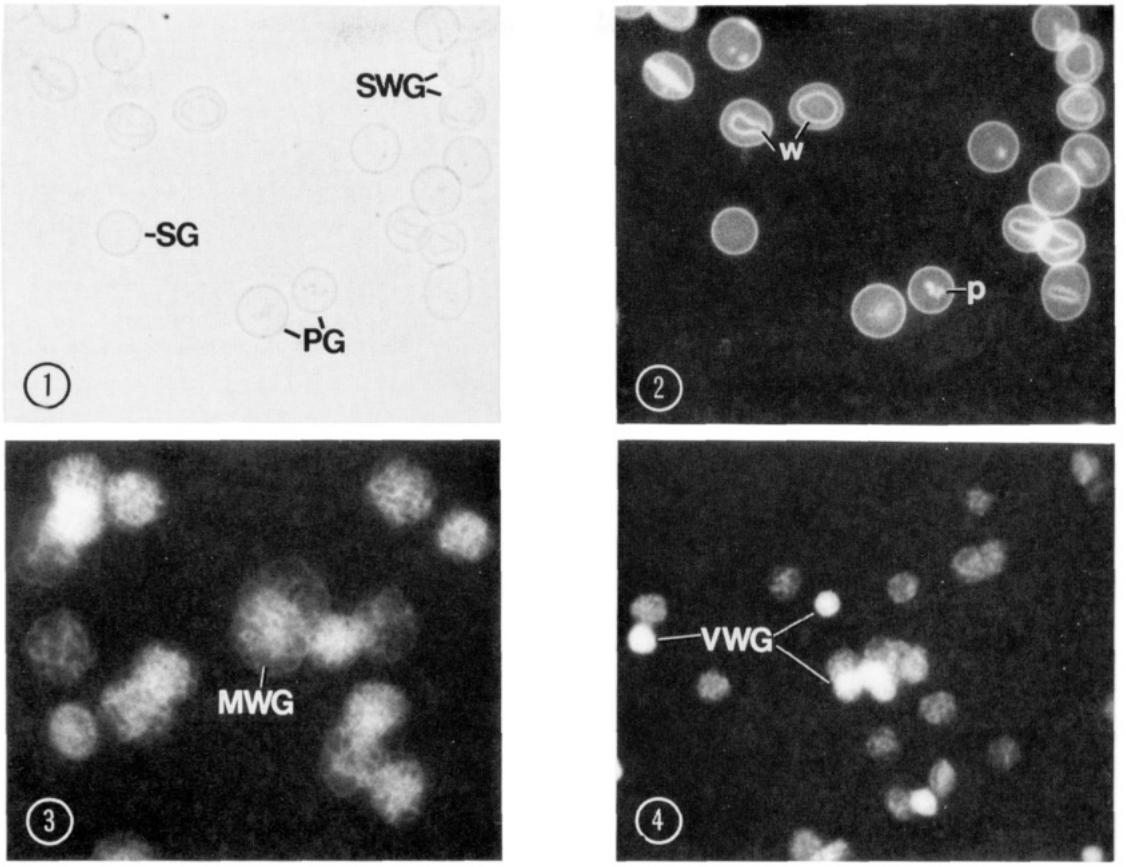

FIGURE 1: Light micrographs of fluorescein thiosemicarbazide labeled RBCs incubated with egg lysoPC for 1 min at 23 °C. Parts 1 and 2 are paired phase contrast and fluorescence micrographs after incubation with 2.1 μg/mL lysoPC, showing smooth ghosts (SGs), single-wrinkle ghosts (SWGs), and patchy ghosts (PGs). Note that the wrinkles (w) are circular in shape and that both the wrinkles and patches (p) are brighter than the surrounding membrane. In part 3 moderately wrinkled ghosts (MWGs) induced by incubation with 4.2 μg/mL lysoPC have a reticular pattern of fluorescence. In part 4 very wrinkled ghosts (VWGs) induced by incubation with 8.4 μg/mL lysoPC are small, tightly folded, and very bright. Parts 1, 2, and 4, 1000×. Part 3, 2000×.

liquid chromatography (HPLC) on an automated gradient system (Waters Associates, Milford, MA). Ghosts were thawed, resuspended in H_2O, and extracted with chloroform/methanol (2:1 v/v) (Folch et al., 1957). The upper phase was discarded and the lower phase dried under N_2. The dried extract was resuspended in chloroform/hexane (1:1 v/v) and injected onto a 5 cm × 4.6 mm guard column packed with Spherisorb 10 μm silica followed by a 10 cm × 4.6 mm HPLC column packed with Spherisorb 3 μm silica (Phenomenex, Rancho Palos Verdes, CA). Lipids were eluted with a ternary gradient as described by Christie (1985). Vessel A contained hexane/tetrahydrofuran (99:1 v/v), vessel B chloroform/2-propanol (1:4 v/v), and vessel C 2-propanol/water (1:1 v/v). The eluate was monitored by a Model 750/14 mass detector (Peris Industries, Inc., State College, PA): the evaporator temperature was 90 °C, and the internal air pressure was 27 psi. The nebulizing gas source was a liquid N_2 (ARLG) tank equipped with a gaseous N_2 outlet and pressure builder. The detector output was digitized by a Model 760 interface (Nelson Analytical, Cupertino, CA) and analyzed with a Vectra computer (Hewlett-Packard, Sunnyvale, CA) using Nelson Analytical 3000 series software. Standard curves were prepared for cholesterol, dioleoylphosphatidylethanolamine, dioleoyl-PC, monooleoyl-PC, phosphatidic acid, phosphatidylserine, and sphingomyelin.

Blood was drawn from four normal individuals for the ghost morphology and lateral mobility studies and from three of these individuals for the lipid composition measurements. Experiments were repeated 2–3 times and the results pooled, since there were no significant differences among results from different donors.

Results

LysoPC Induces Lysis of RBCs and Progressive Folding of RBC Ghost Membranes. The effects of lysoPC incubation on RBC morphology depended on both the concentration of lysoPC and the time of incubation. Low concentrations of egg lysoPC (1.0–1.5 μg/mL) lysed 50% of intact RBCs after a 1-min incubation at 23 °C and 100% of intact RBCs after a 24-h incubation at 37 °C. Higher concentrations of egg lysoPC (>2 μg/mL) lysed 100% of intact RBCs after a 1-min incubation at 23 °C and caused RBC membranes to fragment after a 24-h incubation at 37 °C.

By phase contrast microscopy, ghosts produced by incubation of RBCs with 1–2 μg/mL egg lysoPC for 1 min at 23 °C had three predominant morphologies. First, smooth ghosts (SGs) were 7–8 μm in diameter and had a smooth, unwrinkled contour. Second, single-wrinkle ghosts (SWGs) were 6–8 μm in diameter and had a single circular or elliptical wrinkle in the membrane. Third, patchy ghosts (PGs) were 5–7 μm in diameter and had one to four irregular, 1 μm by 1–3 μm patches of wrinkled membrane. SGs, SWGs, and PGs were all circular or oval in shape (Figure 1). By fluorescence microscopy, the single wrinkles in SWGs and the patches in PGs were brighter than surrounding membrane in ghosts labeled with Fl-PE, fluorescein thiosemicarbazide, or eosin maleimide (Figure 1.2). After incubation of RBCs with 1–2 μg/mL egg lysoPC for 24 h at 37 °C, only SGs and PGs were seen, suggesting that a membrane patch may result from the condensation of a wrinkle.

Table I: Effect of Egg LysoPC on Lateral Mobility of RBC Membrane Components in Smooth and Patchy Ghosts

lysoPC[a] (μg/mL)	morphology[b]	glycophorin			band 3			Fl-PE		
		D[c]	f[d]	n[e]	D[c]	f[d]	n[e]	D[c]	f[d]	n[e]
0	ID	2.6 ± 1.2	50 ± 12	8	1.5 ± 1.0	53 ± 13	8	300 ± 90	96 ± 5	6
0.8	SG	1.0 ± 0.5	44 ± 10	3	1.5 ± 0.1	36 ± 15	3	350 ± 90	94 ± 3	5
	SA/PG	1.7 ± 0.9	41 ± 17	6	1.5 ± 0.1	51 ± 11	3	350 ± 80	94 ± 5	8
	PA/PG	ND[f]	10 ± 8	7	ND[f]	3 ± 5	3	480 ± 90	39 ± 11	8
1.6	SG	2.0 ± 1.2	20 ± 6	4	2.3 ± 0.9	44 ± 11	3	210 ± 50	94 ± 5	6
	SA/PG	2.3 ± 0.1	21 ± 8	2	2.8 ± 0.9	41 ± 18	4	220 ± 60	93 ± 8	8
	PA/PG	ND[f]	6 ± 2	3	ND[f]	2 ± 4	8	350 ± 130	44 ± 13	9

[a] Egg lysoPC was incubated with fluorescently labeled RBCs for 24 h at 37 °C in RPMI, and lateral mobility was measured by FPR, as described under Materials and Methods. [b] ID, intact discocyte; SG, smooth ghost; SA/PG, smooth area of patchy ghost; PA/PG, patchy area of patchy ghost. [c] D, diffusion coefficient, $\times 10^{11}$ cm^2 s^{-1}. Mean ± SD. [d] f, fractional mobility, percent. Mean ± SD. [e] n, number of measurements. [f] ND, not determined for $f < 20\%$.

Incubation of RBCs for 1 min at 23 °C with supralytic concentrations of egg lysoPC (>4 μg/mL) caused progressive wrinkling of ghost membranes. At 4.2 μg/mL lysoPC moderately wrinkled ghosts (MWGs) comprised a uniform population of cells, 5–6 μm in diameter, with reticular wrinkling of the surface (Figure 1.3). At 8.4–16.8 μg/mL lysoPC very wrinkled ghosts (VWGs) appeared as tightly folded spheres, 4–5 μm in diameter, which were extremely bright by fluorescence microscopy (Figure 1.4).

LysoPC Causes a Concentration-Dependent Immobilization of RBC Membrane Components. In intact RBCs glycophorin and band 3 had diffusion coefficients (D's) of 1–3 × 10^{-11} cm^2 s^{-1} and fractional mobilities (f's) of 50–53%. Control values for Fl-PE were $D = 3 \times 10^{-9}$ cm^2 s^{-1} and $f = 96\%$ (Table I). The first set of FPR experiments was performed on SGs and PGs produced by incubation of RBCs with 0.8–1.6 μg/mL egg lysoPC for 24 h at 37 °C. PGs presented an opportunity to measure protein and lipid mobility in two different morphologic regions in the same ghost membrane. In FPR studies on PGs, the laser beam was centered either directly over the patches or over smooth membrane away from the patches (see Figure 1.2). The D and f values of glycophorin, band 3, and Fl-PE in SGs and smooth areas of PGs were not significantly different from those in control RBCs ($p > 0.05$; Student 2-tailed t-test), except that the glycophorin f value was reduced to 20–21% in SGs and smooth areas of PGs produced by incubation with 1.6 μg/mL lysoPC ($p < 0.001$). The Fl-PE D value was significantly greater in patchy than in smooth areas of PGs ($p < 0.05$) (Table I), although it is possible that the "infinite plane" approximation used in calculating D is invalid in patchy areas of PGs. Glycophorin and band 3 were both completely immobilized ($f \leq 10\%$), and Fl-PE was approximately 40% mobile in patchy areas of PGs. Thus, patchy areas of PGs had significantly lower protein and lipid f values than smooth areas.

The second set of FPR experiments was performed on lysoPC-treated RBCs that exhibited progressive membrane wrinkling, i.e., on SWGs, MWGs, and VWGs. In these studies the laser beam was centered over smooth membrane away from the prominent wrinkle on SWGs and over the center of the cell on MWGs and VWGs (see parts 2–4 of Figure 1). As the concentration of egg lysoPC was increased from 0 to 8.4 μg/mL in a 1-min incubation at 23 °C, there was a monotonic decrease in the glycophorin f value. Complete immobilization of both glycophorin and band 3 was observed at a lysoPC concentration of 8.4 μg/mL [Figure 2; Table IV of Golan et al. (1986)]. The Fl-PE f value decreased monotonically over the same concentration range, although approximately 40% of the lipid probe remained mobile at a lysoPC concentration, 8.4 μg/mL, that totally immobilized the transmembrane proteins. A higher concentration of egg lysoPC, 16.8 μg/mL, induced complete immobilization of the lipid probe as well (Figure 2). Thus, progressive immobilization of both protein and lipid correlated with increased wrinkling of the membrane, shown in Figure 1, from intact discocytes to SWGs to MWGs to VWGs.

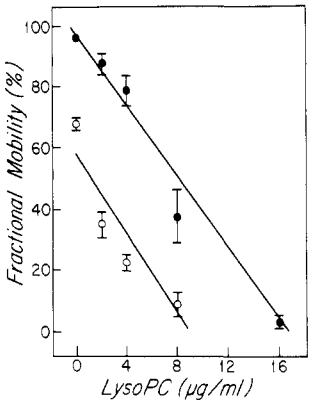

FIGURE 2: Fractional mobility of glycophorin (○) and Fl-PE (●) in fluorescently labeled RBCs incubated with egg lysoPC for 1 min at 23 °C, as a function of lysoPC concentration. Error bars represent standard error of the mean (SEM). Data are fitted by linear least-squares analysis. The predominant RBC morphology for each sample is 0 μg/mL lysoPC, intact discocyte; 2.1 μg/mL lysoPC, SWG; 4.2 μg/mL lysoPC, MWG; 8.4 and 16.8 μg/mL lysoPC, VWG (see Figure 1). Data are taken from Table IV of Golan et al. (1986). LysoPC induces a concentration-dependent immobilization of both glycophorin and Fl-PE.

MPPC Induces Fl-PE Immobilization in RBC Membranes. Because egg lysoPC comprises a mixture of several different lysoPC species, synthetic lysoPCs differing in acyl chain length and/or saturation were tested for their ability to immobilize Fl-PE. Labeled RBCs were incubated for 1 min at 23 °C with synthetic lysoPC at a concentration of 10 μg/mL, the egg lysoPC concentration required for ~60% immobilization of Fl-PE (Figure 2). Of the saturated monoacyl-PC series from monolauroyl (C12:0) through monostearoyl (C18:0), only monopalmitoyl- (C16:0) PC immobilized Fl-PE completely in the entire ghost population (Table II). Monolauroyl-PC lysed approximately 50% of RBCs to SGs, but it did not change the D or f values of Fl-PE. Monomyristoyl- (C14:0), monostearoyl-, and monooleoyl- (C18:1) PCs lysed 100% of RBCs and induced populations of SGs, MWGs, and VWGs. SGs manifested Fl-PE D values that were significantly less than control ($p < 0.001$), without significant change in f values. Fl-PE D values in MWGs and VWGs were also significantly decreased, perhaps due in part to the folding of the membranes themselves, which may cause an underestimation of the "true" D value by up to 2-fold (Aizenbud & Gershon, 1982; Dragsten et al., 1979; Wolf et al., 1982). MWGs and VWGs exhibited partial immobilization of Fl-PE. Whereas the degree of ly-

Table II: Effect of Synthetic LysoPCs on Lateral Mobility of Fl-PE in RBC Membranes

lysoPC species[a]	lysoPC (μg/mL)	morphology[b]	D[d]	f[e]	n[f]
none	0	ID	4.7 ± 1.2	95 ± 6	18
C12:0	10	ID + SG[c]	5.6 ± 1.7	98 ● 5	7
C14:0	10	SG (70%)	2.4 ± 0.7	91 ± 8	9
		VWG (30%)	3.0 ± 1.6	37 ± 17	4
C16:0	0.8	ID (50%)	3.3 ± 1.1	94 ± 6	10
		MWG (50%)	4.2 ± 0.8	54 ± 10	8
	5	VWG	1.3 ± 1.2	26 ± 10	8
	10	VWG	ND[g]	2 ± 3	22
C18:0	1	IE	3.0 ± 1.0	94 ± 8	8
	10	MWG	0.9 ± 0.2	75 ± 8	10
	20	VWG	0.9 ± 0.7	75 ± 15	9
C18:1	10	SG (95%)	2.1 ± 0.8	95 ± 9	7
		VWG (5%)	ND[g]	9 ± 10	4

[a] Synthetic lysoPCs were incubated with Fl-PE-labeled RBCs for 1 min at 23 °C in RPMI, and lateral mobility was measured by FPR, as described under Materials and Methods. [b] Numbers in parentheses refer to the fraction of cells in a sample with the indicated morphology. [c] ID and SG manifested identical D and f values under these conditions. ID, intact discocyte; IE, intact echinocyte; SG, smooth ghost; MWG, moderately wrinkled ghost; VWG, very wrinkled ghost. [d] D, diffusion coefficient, $\times 10^9$ cm^2 s^{-1}. Mean ± SD. [e] f, fractional mobility, percent. Mean ± SD. [f] n, number of measurements. [g] ND, not determined for $f < 20\%$.

Table III: Effect of MPPC on Lateral Mobility of Fl-PE in RBC Ghost Membranes

lysoPC[a] (μg/mL)	morphology[b]	D[c]	f[d]	n[e]
0	SG	3.4 ± 1.0	99 ± 4	8
0.8	SG (50%)	2.3 ± 1.5	94 ± 6	8
	MWG (50%)	0.4 ± 0.3	65 ± 24	6
8	VWG	1.2 ± 0.8	24 ± 11	9
16	VWG	ND[f]	2 ± 2	8

[a] MPPC was incubated with Fl-PE-labeled RBC ghosts for 1 min at 23 °C in RPMI, and lateral mobility was measured by FPR, as described under Materials and Methods. [b] Numbers in parentheses refer to the fraction of cells in a sample with the indicated morphology. SG, smooth ghost; MWG, moderately wrinkled ghost; VWG, very wrinkled ghost. [c] D, diffusion coefficient, $\times 10^9$ cm^2 s^{-1}. Mean ± SD. [d] f, fractional mobility, percent. Mean ± SD. [e] n, number of measurements. [f] ND, not determined for $f < 20\%$.

soPC-induced Fl-PE immobilization was strongly dependent on MPPC concentration, this parameter did not change between monostearoyl-PC (MSPC) concentrations of 10 and 20 μg/mL (Table II).

In order to parallel the protocol used for measurements of lipid composition in MPPC-treated RBCs, the effects of MPPC on morphology and lateral mobility were also examined in ghosts produced by hypotonic lysis. MPPC induced progressive membrane wrinkling and a concentration-dependent decrease in Fl-PE D and f values in hypotonic ghosts (Table III). These effects were similar to the wrinkling and immobilization seen in ghosts produced by MPPC treatment of intact RBCs (Table II), suggesting that the effects of MPPC on lateral mobility are independent of the presence of cytoplasmic RBC components such as hemoglobin.

MPPC-Treated RBC Membranes Incorporate MPPC and Selectively Lose Cholesterol. RBC membrane lipids in control and MPPC-treated ghosts were separated and quantified by HPLC (Figure 3). In control ghosts lysoPC comprised 0.2 ± 0.1% of total lipid (Figure 4), and the molar ratio of cholesterol to total phospholipid was 1.0 ± 0.1 (Figure 5). These values, obtained by HPLC methods, are similar to those measured by other techniques (Cooper et al., 1972; Nelson, 1972; Van Deenen & De Gier, 1974). MPPC incorporation into ghost membranes was linearly dependent (r = 0.97) on

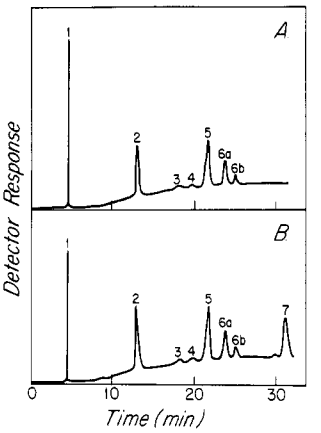

FIGURE 3: HPLC chromatograms of membrane lipids extracted from RBC ghosts incubated with 0 (A) and 16 (B) μg/mL MPPC for 1 min at 23 °C. Peaks, identified by comparison with chromatograms of lipid standards, represent (1) cholesterol, (2) phosphatidylethanolamine, (3) phosphatidic acid, (4) phosphatidylserine, (5) phosphatidylcholine, (6a and 6b) sphingomyelin, and (7) MPPC. MPPC-treated ghosts incorporate MPPC and lose cholesterol. The relative amounts of the major RBC phospholipid classes are unaffected by MPPC treatment.

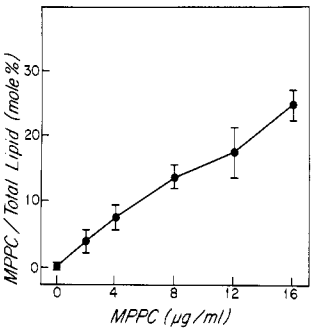

FIGURE 4: MPPC incorporation into RBC ghosts incubated with MPPC for 1 min at 23 °C, as a function of MPPC concentration. Error bars represent standard deviation (SD). MPPC incorporation is linearly dependent on MPPC concentration up to the highest concentration studied.

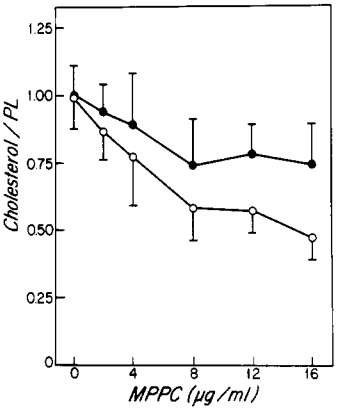

FIGURE 5: Cholesterol/phospholipid molar ratio in RBC ghosts incubated with MPPC for 1 min at 23 °C, as a function of MPPC concentration. The y axis represents cholesterol/(total phospholipid − MPPC) for the upper curve (●) and cholesterol/total phospholipid for the lower curve (○). Error bars represent SD. The cholesterol/phospholipid ratio is inversely dependent on MPPC concentration from 0 to 8 μg/mL and does not change further at 12 and 16 μg/mL.

MPPC concentration. At 16 μg/mL MPPC, the highest concentration studied, lysoPC comprised 25 ± 2% of total membrane lipid (Figure 4). Membrane cholesterol content was inversely dependent on MPPC concentration. The molar ratio of cholesterol to total phospholipid fell to 0.6 ± 0.1 at

Table IV: LysoPC Concentration Required for Lysis of 50% of RBCs

hct (%)	L_{50}[a] (μg/mL)	L_{50}/hct (μg mL^{-1} hct^{-1})	lysoPC species	ref
0.2	1.0–1.5	5.0–7.5	egg lysoPC	this study
0.2	0.8	4.0	MPPC	this study
1	~3	~3	MSPC	Weltzien (1979)
1	4.4	4.4	egg lysoPC	Mitsui et al. (1982)
2	15	7.5	egg lysoPC	Omachi et al. (1982)
50	~250	~5	MPPC	Bierbaum et al. (1979)

[a] L_{50}, lysoPC concentration that lyses 50% of RBCs.

8 μg/mL MPPC and did not decrease further at 12 and 16 μg/mL (Figure 5). The decrease in this ratio was not caused solely by the increase in phospholipid due to membrane incorporation of MPPC, since the molar ratio of cholesterol to phospholipid (exclusive of MPPC) also fell significantly with increasing MPPC concentration. The latter ratio decreased from 1.0 ± 0.1 at 0 μg/mL MPPC to 0.7 ± 0.2 at 8 μg/mL MPPC and did not change further at 12 and 16 μg/mL (Figure 5). Membrane cholesterol was presumably extracted and solubilized by micelles of MPPC.[2] Of note, the molar ratio of MPPC to cholesterol in ghost membranes was ~1 at 16 μg/mL MPPC (Figures 4 and 5), and ghosts fragmented at higher concentrations of MPPC. MPPC treatment did not affect the relative amounts of the major RBC phospholipid classes (Figure 3).

Discussion

These studies demonstrate that supralytic concentrations of lysoPC cause the RBC ghost membrane to form patches and to wrinkle progressively. In patchy ghosts, patches exhibit complete immobilization of glycophorin and band 3 and partial immobilization of Fl-PE, whereas adjacent smooth membrane areas manifest only partial protein immobilization and no Fl-PE immobilization. In wrinkled ghosts, glycophorin and band 3 are completely immobilized at 8.4 μg/mL egg lysoPC, and Fl-PE is completely immobilized at 16.8 μg/mL egg lysoPC. Among the synthetic lysoPCs tested, MPPC, the major component of egg lysoPC, is unique in its ability to immobilize Fl-PE completely. Finally, MPPC-induced wrinkle and patch formation and Fl-PE immobilization appear to be caused by ghost membrane MPPC incorporation and cholesterol depletion.

The concentration of lysoPC required for lysis of 50% of RBCs (i.e., the L_{50}) is dependent on both the absolute concentration of lysoPC and the concentration of RBCs in suspension [i.e., the hematocrit (hct)]. When the L_{50} is normalized by the RBC concentration, our values for L_{50}/hct, 5.0–7.5 μg of egg lysoPC mL^{-1} hct^{-1} and 4 μg of MPPC ml^{-1} hct^{-1}, compare favorably with literature values (Table IV). Since both the RBC and the lysoPC concentration are important in determining the L_{50}, lysis appears to be governed by the lysoPC partition coefficient between aqueous phase and RBC membrane and not by the cmc of lysoPC in aqueous solution.[2]

On the basis of the data in Table III and Figure 4 and the calculation[3] that the native RBC membrane contains ~4 × 10^8 lipid molecules, we find that ~8 × 10^6 MPPC molecules/RBC are needed for lysis [see also Weltzien et al. (1977)] and ~1 × 10^8 molecules/RBC for Fl-PE immobilization. In comparison, ~2–4 × 10^6 MPPC molecules/RBC are needed to produce echinocytes (Fujii & Tamura, 1983; Lange & Slayton, 1982; Mohandas et al., 1978). Echinocytosis, lysis, membrane folding, and membrane lipid immobilization are therefore associated with the membrane incorporation of ~1, ~2, ~2–12, and ~25 mol % MPPC relative to total RBC lipid, respectively.

MPPC is similar to egg lysoPC in its ability to immobilize Fl-PE completely. In contrast, the f value of Fl-PE is affected only mildly by concentrations of MSPC that are well above the cmc for this species.[2] The difference between the effects of MPPC and MSPC on Fl-PE mobility is striking, since MPPC and MSPC have similar binding affinities for RBC membranes [reviewed in Weltzien (1979)]. Since egg lysoPC is comprised of 70.5% MPPC and 25.7% MSPC, MPPC is most likely the component of egg lysoPC responsible for RBC membrane protein and lipid immobilization. Further, both MPPC and MSPC induce membrane wrinkling, yet only MPPC induces complete Fl-PE immobilization. Wrinkling may be a direct consequence of lysoPC binding to RBCs, but factors in addition to binding may be necessary for immobilization. Such factors could include the molecular composition and organization of lysoPC-induced lipid domains (see below).

Fl-PE immobilization is associated not only with MPPC incorporation but also with cholesterol extraction from ghost membranes. Fl-PE mobility and MPPC incorporation both change significantly, however, over an MPPC concentration range in which the cholesterol/phospholipid ratio remains constant (Figures 4 and 5). It is therefore unlikely that cholesterol depletion alone is responsible for lipid probe immobilization. This conclusion is supported by the finding that the f value of a carbocyanine dye remains high, 85–100%, in cholesterol-depleted ghosts (Thompson & Axelrod, 1980). Our observation that MPPC-treated ghosts fragment at MPPC/cholesterol molar ratios >1 suggests that there may be an affinity between MPPC and membrane cholesterol. In model systems, 1:1 molar ratios of lysoPC and cholesterol produce gel-phase bilayers in aqueous solution (Rand et al., 1975; van Echteld et al., 1981).

The hypothesis that lipid domains form in MPPC-treated ghosts explains both the membrane deformations and the immobilization of Fl-PE seen in these membranes. Such domains are not present in untreated RBC membranes (Golan et al., 1984; Golan & Veatch, 1980; Gottlieb & Eanes, 1974; Karnovsky et al., 1982; Kinosita et al., 1981; Klausner et al., 1980; Ladbrooke & Chapman, 1969), in which Fl-PE is 90–100% mobile. The clearest demonstration of domain formation is provided by PGs. Since smooth and patchy areas of PGs manifest different f values, they must represent regions that are inhomogeneous with respect to composition and/or organization. Lipid probe immobilization in wrinkled ghosts, like that seen in other model (Klausner & Wolf, 1980) and biological (Yechiel & Edidin, 1987; Metcalf et al., 1986; Wolf et al., 1981) membranes, is also explained by domain formation. LysoPC-induced lipid domains have been suggested by ultrastructural studies showing scalloping and membrane discontinuities in RBC ghosts produced by lysoPC treatment (Seeman, 1967) and clustering of cationized ferritin binding

[2] The critical micelle concentration (cmc) of MPPC in aqueous solution is 7 μM, or 3.5 μg/mL (Haberland & Reynolds, 1975). Although the cmc of MSPC in aqueous solution has not been determined experimentally, theoretical considerations [reviewed in Weltzien (1979)] suggest that this value should be ~1 order of magnitude less than that of MPPC, or ~0.4 μg/mL.

[3] The number of lipid molecules per RBC was calculated by assuming an RBC surface area of 150 μm^2, of which lipid occupies an area fraction of 0.83 (Golan et al., 1984), and a phospholipid or cholesterol surface area of 70 Å^2.

sites on lysoPC-induced echinocytes (Marikovsky et al., 1976). Lipid domain formation has also been invoked as the mechanism by which lysoPC lyses membranes (Lee & Chan, 1977; Weltzien et al., 1976; Weltzien, 1979), shifts membrane phase transition temperatures (Blume et al., 1976), and increases membrane permeability [reviewed in Weltzien (1979)].

The nature of MPPC-induced domains remains to be elucidated. Physically, the diameter of these domains must be <1 μm in order to produce complete Fl-PE immobilization (Klausner & Wolf, 1980; Owicki & McConnell, 1980; Yechiel & Edidin, 1987). Chemically, these domains may consist of lysoPC- and cholesterol-rich gel-phase lipid (see above). Coexisting immiscible fluid-phase domains (Recktenwald & McConnell, 1981), nonbilayer phase domains (Bangham & Horne, 1964; Hui et al., 1983; Inoue et al., 1977), and intramembranous domains of pure lysoPC (Lucy, 1970) are also possible. Domain formation by any of these mechanisms could account for the effects of lysoPC on biological membranes, including permeability changes (Lee & Chan, 1977), fusion (Lucy, 1970), alterations in membrane protein function (Miyahara et al., 1981), and fusion and lysis of host blood cells adherent to schistosomula (Caulfield et al., 1980; Golan et al., 1986). Both the molecular species of the lysoPC and the composition and organization of the biological membrane may determine the selective effects of lysoPC on membranes.

ACKNOWLEDGMENTS

We thank Catherine M. L. Cianci and Yung J. Han for excellent technical assistance and Ann Hein for critical review of the manuscript.

REFERENCES

Aizenbud, B. M., & Gershon, N. D. (1982) *Biophys. J. 38*, 287–293.

Axelrod, D., Koppel, D. E., Schlessinger, J., Elson, E., & Webb, W. W. (1976) *Biophys. J. 16*, 1055–1069.

Bangham, A. D., & Horne, R. W. (1964) *J. Mol. Biol. 8*, 660–668.

Bierbaum, T. J., Bouma, S. R., & Huestis, W. H. (1979) *Biochim. Biophys. Acta 555*, 102–110.

Blume, A., Arnold, B., & Weltzien, H. U. (1976) *FEBS Lett. 61*, 199–202.

Caulfield, J. P., & Cianci, C. M. L. (1985) *J. Cell Biol. 101*, 158–166.

Caulfield, J. P., Korman, G., Butterworth, A. E., Hogan, M., & David, J. R. (1980) *J. Cell Biol. 86*, 46–63.

Christie, W. W. (1985) *J. Lipid Res. 26*, 507–512.

Cooper, R. A., Diloy-Puray, M., Lando, P., & Greenberg, M. S. (1972) *J. Clin. Invest. 51*, 3182–3192.

Dragsten, P., Henkart, P., Blumenthal, R., Weinstein, J., & Schlessinger, J. (1979) *Proc. Natl. Acad. Sci. U.S.A. 76*, 5163–5167.

Folch, J., Lees, M., & Sloan-Stanley, G. H. (1957) *J. Biol. Chem. 226*, 497–509.

Fujii, T., & Tamura, A. (1983) *Biomed. Biochim. Acta 42*, S81–S85.

Golan, D. E., & Veatch, W. (1980) *Proc. Natl. Acad. Sci. U.S.A. 77*, 2537–2541.

Golan, D. E., Alecio, M. R., Veatch, W. R., & Rando, R. R. (1984) *Biochemistry 23*, 332–339.

Golan, D. E., Brown, C. S., Cianci, C. M. L., Furlong, S. T., & Caulfield, J. P. (1986) *J. Cell Biol. 103*, 819–828.

Gottlieb, M. H., & Eanes, E. D. (1974) *Biochim. Biophys. Acta 373*, 519–522.

Haberland, M. E., & Reynolds, J. A. (1975) *J. Biol. Chem. 250*, 6636–6639.

Hui, S. W., Stewart, T. P., & Boni, L. T. (1983) *Chem. Phys. Lipids 33*, 113–126.

Inoue, K., Suzuki, K., & Nojima, S. (1977) *J. Biochem. (Tokyo) 81*, 1097–1106.

Karnovsky, M. J., Kleinfeld, A. M., Hoover, R. L., & Klausner, R. D. (1982) *J. Cell Biol. 94*, 1–6.

Kinosita, K., Kataoka, R., Kimura, Y., Gotoh, O., & Ikegami, A. (1981) *Biochemistry 20*, 4270–4277.

Klausner, R. D., & Wolf, D. E. (1980) *Biochemistry 19*, 6199–6203.

Klausner, R. D., Kleinfeld, A. M., Hoover, R. L., & Karnovsky, M. J. (1980) *J. Biol. Chem. 255*, 1286–1295.

Ladbrooke, B. D., & Chapman, D. (1969) *Chem. Phys. Lipids 3*, 304–367.

Lange, Y., & Slayton, J. M. (1982) *J. Lipid Res. 23*, 1121–1127.

Lee, Y., & Chan, S. I. (1977) *Biochemistry 16*, 1303–1309.

Lucy, J. A. (1970) *Nature (London) 227*, 814–817.

Marikovsky, Y., Brown, C. S., Weinstein, R. S., & Wortis, H. H. (1976) *Exp. Cell Res. 98*, 313–324.

Metcalf, T. N., Wang, J. L., & Schindler, M. (1986) *Proc. Natl. Acad. Sci. U.S.A. 83*, 95–99.

Mitsui, K., Saeki, Y., & Hase, J. (1982) *Biochim. Biophys. Acta 686*, 177–181.

Miyahara, M., Nishihara, Y., Morizimato, Y., & Utsumi, K. (1981) *Biochim. Biophys. Acta 641*, 232–241.

Mohandas, N., Greenquist, A. C., & Shohet, S. B. (1978) *J. Supramol. Struct. 9*, 453–458.

Nelson, G. J. (1972) *Blood Lipids and Lipoproteins: Quantitation, Composition, and Metabolism*, Wiley-Interscience, New York.

Omachi, A., Sarpel, G., Podolski, J. L., Barr, A. N., Lazowski, E., & Danon, M. J. (1982) *J. Neurol. Sci. 56*, 249–258.

Owicki, J. C., & McConnell, H. M. (1980) *Biophys. J. 30*, 383–398.

Rand, R. P., Pangborn, W. A., Purdon, A. D., & Tinker, D. O. (1975) *Can. J. Biochem. 53*, 189–195.

Recktenwald, D. J., & McConnell, H. M. (1981) *Biochemistry 20*, 4505–4510.

Seeman, P. (1967) *J. Cell Biol. 32*, 55–70.

Thompson, N. L., & Axelrod, D. (1980) *Biochim. Biophys. Acta 597*, 155–165.

Van Deenen, L. L. M., & De Gier, J. (1974) in *The Red Blood Cell* (Surgenor, D. M., Ed.) pp 147–211, Academic, New York.

Van Echteld, C. J. A., De Kruijff, B., Mandersloot, J. G., & De Gier, J. (1981) *Biochim. Biophys. Acta 649*, 211–220.

Weltzien, H. U. (1979) *Biochim. Biophys. Acta 559*, 259–287.

Weltzien, H. U., Arnold, B., & Kalkoff, H. G. (1976) *Biochim. Biophys. Acta 455*, 56–65.

Weltzien, H. U., Arnold, B., & Reuther, R. (1977) *Biochim. Biophys. Acta 466*, 411–421.

Wolf, D. E., Kinsey, W., Lennarz, W., & Edidin, M. (1981) *Dev. Biol. 81*, 133–138.

Wolf, D. E., Handyside, A. H., & Edidin, M. (1982) *Biophys. J. 38*, 295–297.

Yechiel, E., & Edidin, M. (1987) *J. Cell Biol. 105*, 755–760.